123

MECHANOCHEMICAL COUPLING IN ATPASE MOTORS

Charles S. Peskin
Courant Institute of Mathematical Sciences, 251 Mercer Street, New York, NY 10012.
peskin@cims.nyu.edu

George Oster
Department of Molecular and Cellular Biology, University of California, Berkeley, CA 94720.
goster@nature.berkeley.edu

IN: *Interplay of Genetic and Physical Processes in the Development of Biological Form.* Les Éditions de Physique (F. Dykstra, D. Beysens, M.-A. Felix, G. Gorgacs, F. Gaill, Eds.). New York: Springer-Verlag (1994).

1. INTRODUCTION

Many molecular motors share three characteristics in their operation. First, they move unidirectionally along a polymer ligand (Walker et al., 1990; Schafer et al., 1991; Sheetz et al., 1991). Second, they employ a nucleotide hydrolysis cycle as their energy source. Third, they are multimeric ATPases; that is, they are composed of several subunits, each of which contains one or more nucleotide hydrolysis sites. We shall demonstrate that these properties suffice to drive a unidirectional molecular motor providing that the ATPase activities of the various sites are correlated. This is a novel mechanism for transducing phosphate bond energy into directed motion, and it is likely to play a role in a wide variety of "processive" enzymes, such as polymerases (Schafer, Gelles et al., 1991), chaperonins (Ellis, 1993), as well as the conventional motors, myosin, dynein and kinesin. We shall use as an example the transduction of free energy by the motor molecule kinesin, since the mechanical behavior of single kinesin molecules has recently been measured (Svoboda et al., 1993).

2. MOTORS DRIVEN BY REACTION ASYMMETRY

The essential mechanical feature of a motor's nucleotide hydrolysis cycle is that it alternates binding affinity of the motor for its track between strong and weak binding configurations (Eisenberg et al., 1985; Ellis, 1993). In this section we desecribe two motor models whose functioning depends on the fact that their overall reaction rates reflect the activities of different ATPase sites. For simplicity, we will restrict ourselves to motors with 2 enzymatic sites which are elastically coupled. We begin with a model in which the hydrolysis reactions strictly alternate, implying a complete coordination between the reaction sites. Then we progress to a model in which the reactions are not alternating, but where there is a net difference in reaction rates between the two sites.

2.1 A simple stochastic model with alternating reaction rates

Consider a macromolecular enzyme consisting of two parts that are rigidly connected (i.e. a 2-legged motor) that moves on a double potential track, as shown in Figure 1a. We suppose that the enzyme can bind alternately to one or the other track by alternating its ATPase activity. Figure 1b illustrates how the motor operates. The motor has two binding sites, each equipped with a nearby ATPase site. In state 1, the motor is bound on one track. The ATPase cycle dissociates the motor from this binding site, bringing the other site within binding range of the other track. (As with other molecular motors (e.g. kinesin, myosin), the binding is predominantly electrostatic, so that the complementary sites must approach to within a Debye length to 'see' one another.) In effect, this 'lifts' the state from 1→ 2, so the motor's other active site finds itself on the potential slope of the other DNA strand. Now it 'slides' down the potential gradient until it reaches the minimum at state 3, whereupon its ATPase dissociates it and reseats the opposing component of the motor on the first track at state 4. In this fashion, the motor is always sliding down one or the other potential surface to a local minimum; work is performed by the ATPase reactions which dissociate the motor from one minimum and transfer it to the other. Note that the motor moves in the opposite direction as would a macroscopic ratchet.

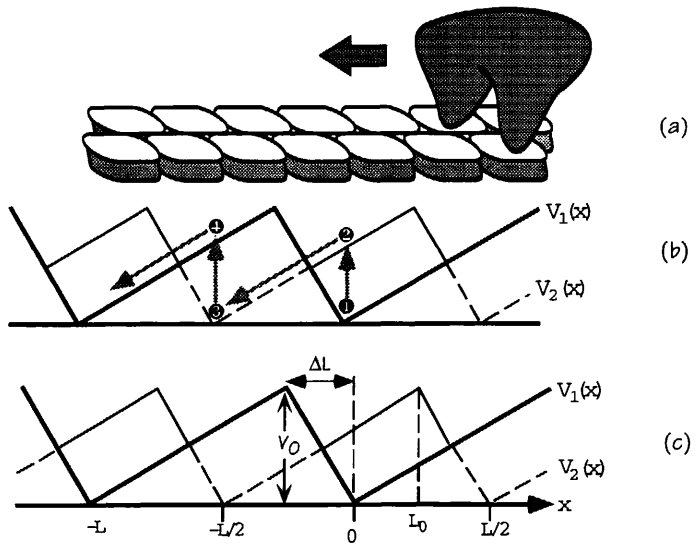

Figure 1. (a) A progressive ATPase with two reaction sites rigidly coupled 'walks' to the left along a double track of binding sites. The sites are staggered as shown in (b). (b) The path of the system through the sequence of states 1 → 4, where the transitions 1 → 2 and 3 → 4 are the ATPase-driven dissociation from one track and binding to the other track. Transition 2 → 3 is diffusion down the potential gradient. (c) Notation used in the text.

We can write the equations governing the motor as follows. We label the potential locations as shown in Figure 1c, and consider an ensemble of points diffusing on the potential surface. Let $c_1(x)$, $c_2(x)$ be the concentration of points in potential 1 and 2, respectively. The steady state diffusion equations are:

$$\frac{d}{dx}\phi_1 = \gamma(c_2 - c_1)$$
$$\frac{d}{dx}\phi_2 = \gamma(c_1 - c_2) \qquad (1)$$

where the fluxes are

$$\phi_i = -D\frac{dc_i}{dx} - \frac{D}{k_BT}\left(\frac{dV_i}{dx}\right)c_i,\ i = 1,2 \qquad (2)$$

Since, in the steady state $c(x) = c(x + L)$, we expect solutions in which $c_2(x + L/2) = c_1(x)$, and $c_1(x + L/2) = c_2(x)$. Thus we can restrict our attention to the interval (0,L/2) and impose the following boundary conditions:

$$c_2(L/2) = c_1(0), \qquad c_1(L/2) = c_2(0) \qquad (3a,b)$$

Let $L_0 = L/2 - \Delta L$ (see Figure 1c). Then

$$c_1(L_0^-) = c_1(L_0^+)$$
$$c_2(L_0^-) = c_2(L_0^+) \qquad (4)$$

The fluxes, $\phi_i(x)$ are continuous, even when $V'(x)$ is not; thus at $x = L_0$:

$$\frac{dc_1}{dx}(L_0^-) = \frac{dc_1}{dx}(L_0^-) \qquad (5)$$

since $V_1'(x)$ is continuous at L_0, and

$$\frac{dc_2}{dx}(L_0^-) + \frac{V_0}{k_BT(L-\Delta L)}c_2(L_0^-) = \frac{dc_2}{dx}(L_0^+) - \frac{V_0}{k_BT\Delta L}c_2(L_0^+) \qquad (6)$$

Similarly, at $x = 0$, we have

$$\frac{dc_1}{dx}(0^-) - \frac{V_0}{k_BT\Delta L}c_1(0) = \frac{dc_1}{dx}(0^+) + \frac{V_0}{k_BT(L-\Delta L)}c_1(0)$$
$$\frac{dc_2}{dx}(0^-) = \frac{dc_2}{dx}(0') \qquad (7)$$

As a specific example of this type of motor, consider an RNA polymerase motor translocating along its DNA track. Figure 2a shows the strands 'unraveled' to expose the two tracks. The model equations can be solved numerically to produce the force-velocity relationship shown in Figure 2b. The velocity is in the range of that observed for polymerases, and the work it is capable of performing is comparable to thermal energies.

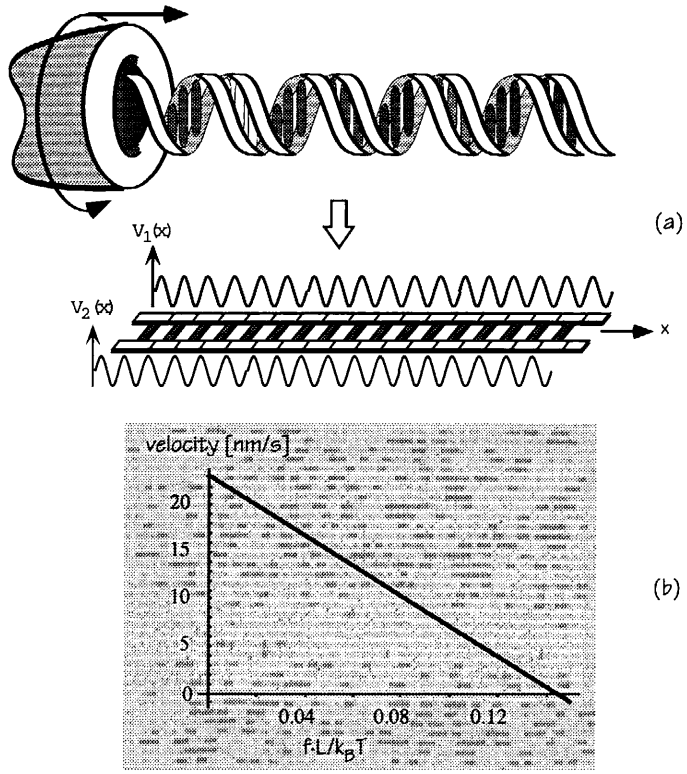

Figure 2: (a) Schematic diagram of an RNA polymerase progressing along DNA. We suppose that the polymerase encircles the DNA so as to obviate dissociation, and that it translates and rotates with respect to the track. (b) Computed load-velocity curve using parameters typical of RNA polymerase: $V_{max} = 3$ k_BT, L = 3.4 nm, ΔL = 0.6 nm, hydrolysis rate = 100/s, diffusion coefficient = 5×10^3 nm^2/s. (Note that since the motor moves to the left, we have plotted velocity is positive to the left and load force as positive to the right.)

2.2 A model with asynchronous reaction rates

In this model we investigate the consequences of a simple interaction between the motor heads which allows them to operate asynchronously. We assume that only one head can bind to each site at a time and that the heads are hinged but their motion restricted so that the distance between the heads is at most L = 8 nm, the distance between binding sites. We also assume that each head has a "watchspring" at its "ankle" hinge that provides a passive elastic restoring force to an equilibrium position with respect to the track (c.f. Figure 3).

The asymmetry is introduced as follows. Each head has an independent ATPase site, but they are located such that the back head is more likely to bind and hydrolyze an ATP. We shall simplify each hydrolysis cycle to a 2-state Markov chain. In the unbound state a head can diffuse rapidly within the interval (-L, L) with respect to the other (bound) head. Upon completion of the hydrolysis cycle (e.g. release of ADP in kinesin) the head re-acquires a strong-binding affinity. Since the diffusion is so rapid compared with the chemical cycle, the head immediately binds to one of the sites at $\pm L$ with respect to the other head. With no loading, the binding sites at $\pm L$ are equally likely. However, in the presence of a load, f, binding is more likely on the left. Thus the load influences the mean velocity of the motor.

Let β be the rate constant for the transition (release of P_i) to the weakly bound state (0), and α the transition rate (release of ADP) for rebinding to the fiber, (state 1). The key assumption in this model is that β is different for the two heads:

β_1 = rate constant for the back head $1 \rightarrow 0$

β_2 = rate constant for the front head $1 \rightarrow 0$,

α = rate constant for both heads $0 \rightarrow 1$

The asymmetry contained in the inequality $\beta_2 < \beta_1$ is what drives the motor forward. We analyze the situation as follows.

The mean waiting time in state (1, 1) (i.e. both heads bound) is

$$\langle T_{bound} \rangle = \frac{1}{\beta_1 + \beta_2} \tag{8}$$

The random variable T_{bound} is *independent* of which head lifts. Then the mean time in the weakly bound state is

$$\langle T_{free} \rangle = \frac{1}{\alpha} \tag{9}$$

Thus the mean cycle time is

$$\langle T_{cycle} \rangle = \frac{1}{\beta_1 + \beta_2} + \frac{1}{\alpha} \tag{10}$$

Denote the load by f and define

p(f) = probability that the free head eventually binds at the site which is *ahead* of the bound head

1 - p(f) = probability that the free head eventually binds *behind* the bound head.

The form of p(f) will be determined below; clearly, it is monotonically decreasing. The probabilities for different cycle outcomes can be read from the following diagram:

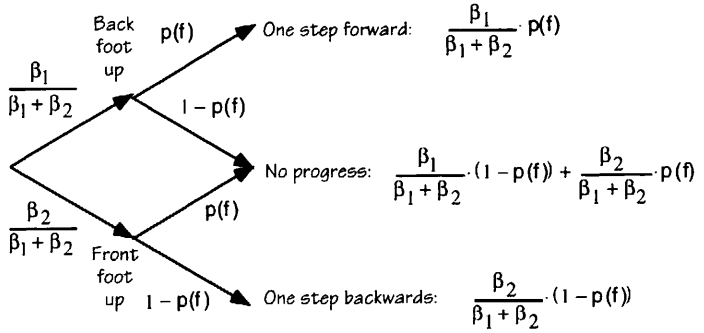

From the diagram we can express the mean distance traveled forward per cycle as

$$\begin{aligned}\langle X_{cycle}\rangle &= \frac{\beta_1}{\beta_1+\beta_2}\cdot p(f)\cdot L + \frac{\beta_2}{\beta_1+\beta_2}\cdot(1-p(f))\cdot(-L)\\ &= \frac{\beta_1 p(f)-\beta_2(1-p(f))}{\beta_1+\beta_2}\cdot L = \left[p(f)-\frac{\beta_2}{\beta_1+\beta_2}\right]\cdot L\end{aligned} \tag{11}$$

Note that ,since the waiting time is each state is a Markov process, independent of the path taken to leave that state, X_{cycle} and T_{cycle} are independent random variables. Moreover, each cycle is independent of the others. Now consider N successive cycles resulting in displacement X over time T:

$$\frac{X}{T} = \frac{X_{cycle}^{(1)}+\cdots+X_{cycle}^{(N)}}{T_{cycle}^{(1)}+\cdots+T_{cycle}^{(N)}}$$

Since X and T are independent

$$\left\langle\frac{X}{T}\right\rangle = \frac{\left\langle X_{cycle}^{(1)}+\cdots+X_{cycle}^{(N)}\right\rangle}{\left\langle T_{cycle}^{(1)}+\cdots+T_{cycle}^{(N)}\right\rangle} = \frac{N\langle X_{cycle}\rangle}{N\langle T_{cycle}\rangle} = \langle v\rangle$$

Thus we can express the mean velocity as

$$\langle v\rangle = \frac{\langle X_{cycle}\rangle}{\langle T_{cycle}\rangle} = \frac{\left[p(f)-\frac{\beta_2}{\beta_1+\beta_2}\right]L}{\frac{1}{\beta_1+\beta_2}+\frac{1}{\alpha}} = \frac{(\beta_1+\beta_2)L\left[p(f)-\frac{\beta_2}{\beta_1+\beta_2}\right]}{1+\frac{\beta_1+\beta_2}{\alpha}} \tag{12}$$

In order to compute the force velocity curve we write the dependence of the β's on ATP as $\beta_1 = \beta_1^0 g([ATP])$, $\beta_2 = \beta_2^0 g([ATP])$, $\beta_1^0 > \beta_2^0$. Then the expression for the velocity as a function of load, f, and ATP concentration is:

$$\langle v(f,ATP)\rangle = g([ATP])\frac{(\beta_1^0+\beta_2^0)L}{1+\frac{\beta_1^0+\beta_2^0}{\alpha}g([ATP])}\cdot\left(p(f)-\frac{\beta_2^0}{\beta_1^0+\beta_2^0}\right) \tag{13}$$

In order to compute p(f) we solve the following problem. For $t < 0$, a particle diffuses in a potential $\phi(x)$ on the interval (-L, L) with reflecting boundaries. Then, at $t = 0$, the ends of the interval switch to become absorbing boundaries. We calculate the probability that the particle is absorbed at the right end of the interval. The result is (Weiss, 1967; Lindenberg et al., 1979)

$$p_L(f) = \frac{\int_{-L}^{L} e^{\phi(x,f)/k_BT}\left[\int_{-L}^{x}\rho_0(x')dx'\right]dx}{\int_{-L}^{L} e^{\phi(x,f)/k_BT}dx} \tag{14}$$

Here $\rho_0(x)$ is the equilibrium distribution $\rho_0(x) = e^{-\phi(x)/k_BT}/\int_{-L}^{L} e^{-\phi(x')/k_BT}dx'$, and the potential $\phi(x)$ is given by

$$\phi(x,f) = \frac{f\cdot x}{2} + \frac{K(x-x_0)^2}{2} \tag{16}$$

where the first term is the potential due to the load. The factor 1/2 arises because the hinge at which the load is applied moves only half as far as the free foot. The second term is the potential due to the (effective) spring connecting the two heads. (Note that when $x_0 > 0$ the heads have unequal binding probability even at no load. This offset was necessary to fit the data.) The general shape of p(f) is sigmoidal.

From equation (14), we see that the stall force is given by

$$p(f_0) = \frac{\beta_2^0}{\beta_1^0+\beta_2^0} < \frac{1}{2} \tag{17}$$

which is independent of the ATP concentration (c.f. Svoboda & Block, 1994). As [ATP] changes, the force-velocity relation scales on the velocity axis. Figure 3b,c shows fits of the model to the load velocity data at high (2 mM) and low (10μM) ATP concentrations.

A possibly better model for RNA polymerase is shown below. This is based on the same principle of correlated hydrolysis as kinesin, but this is a 'shuffle-walker', rather than a hand-over-hand walker. That is, the front subunit hydrolyzes faster than the back subunit (e.g. by site occlusion), so the motor moves forward like in 'inchworm'.

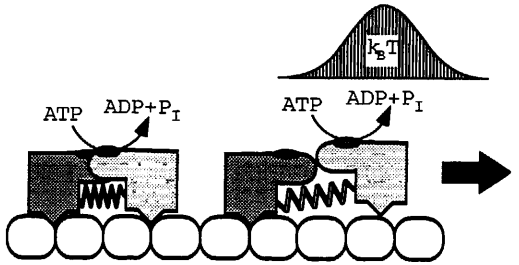

Figure 3. An alternative model for an RNA polymerase. Left panel: the front subunit occludes the rear subunit, and so binds ATP and detaches from the track first. Thermal fluctuations carry it to the next site where it binds, and the rear subunit binds ATP, releases and diffuses forward. The force-velocity curve is similar to that computed for kinesin; however, in this model, with no conformational change, a maximum of 1-2 pN of thrust is possible.

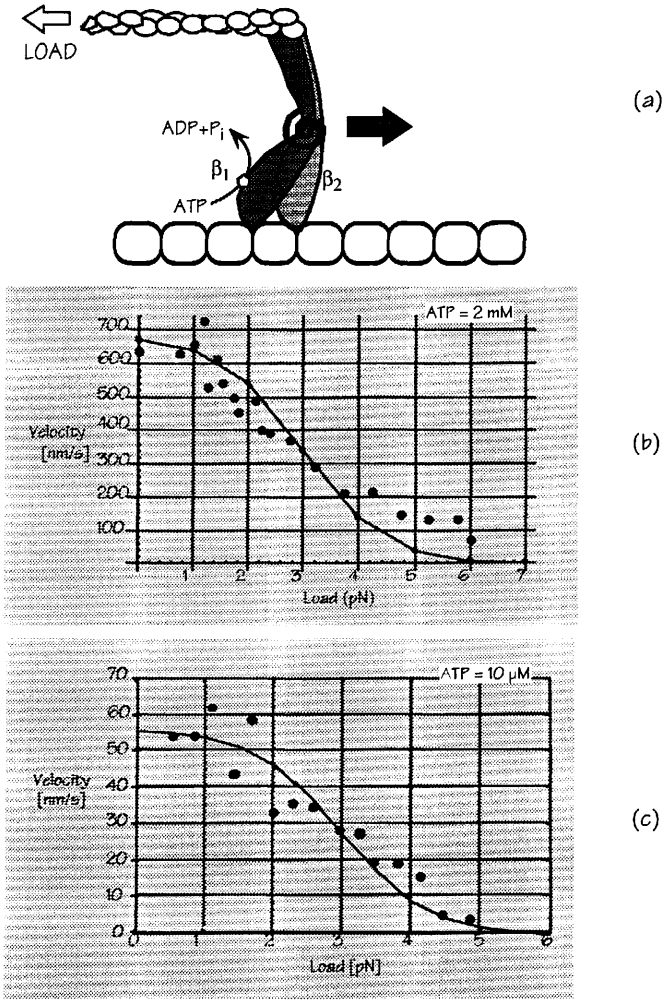

Figure 3: (a) Schematic of a kinesin motor. The rear head hydrolyzes ATP faster than the front head: $\beta_1 > \beta_2$. Comparison of the model (solid line) with the data of Svoboda & Block (1994) at high ATP concentration (b) and low ATP concentraion (c).

3. Discussion

The principle enunciated here is simple: a pair of elastically coupled ATPases can function as a powerful Brownian motor providing the hydrolysis rates of the two sites are different. The motors 'walk' on a track with periodically spaced binding sites. The rearmost ATPase of a 'hand-over-hand walker' runs faster, while the foremost ATPase in a 'shuffle walker' runs faster. Thus the motor alternates between a 'contracted' and an 'expanded' state to stochastically walk along its polymer track.

We suggest two mechanisms for this differential reaction rate. The two components of the motor may fit together in such a manner that one ATPase site occludes the other in the contracted state. Alternatively, the strain state of the components may be such that in the contracted state one of the ATPase sites is deformed so as to reduce its affinity for nucleotide, or its capacity to hydrolyze bound nucleotide.

Several authors have proposed models for molecular motors based on biasing Brownian motion (Astumian et al., 1993; Peskin et al., 1993; Prost et al., 1994; Peskin et al., 1994; Doering et al., 1994). The difficulty has been not in matching the observed velocities, but in generating the piconewton forces measured in optical trap assays (Svoboda et al., 1994; Finer et al., 1994). The mechanism we propose here fits the measured force-velocity curves for kinesin quite well, over a wide range of ATP concentrations. In view of the fact that all known molecular motors are multimeric, multi-ATPases, we suggest that the principle outlined here may apply to other progressive enzymes, such as DNA and RNA polymerases (Schafer, Gelles et al., 1991), chaperonins (Ellis, 1993), as well as the more familiar 'walking' enzymes, myosin, kinesin, and dynein.

Acknowledgements

CSP and GFO were supported by Grant No. NSF FD92-20719 from the National Science Foundation. The authors would like to thank Karel Svoboda and Steve Block for sharing their data with us prior to its publication.

References

Weiss, G. (1967). First passage time problems in chemical physics. Adv. Chem. Phys. **13**:1-18.

Lindenberg, K. V. Seshadri (1979). Analytic theory of extrema. I. Asymptotic theory for Fokker-Planck processes. J. Chem. Phys. **71**:4075-4084.

Eisenberg, E. T. Hill (1985). Muscle contraction and free energy transduction in biological systems. Science. **227**:999-1006.

Walker, R., E. Salmon S. Endow (1990). The Drosophila claret segregation protein is a minus-end directed motor molecule. Nature. **347**:780-782.

Schafer, D.A., J. Gelles, M.P. Sheetz R. Landick (1991). Transcription by single molecules of RNA polymerase observed by light microscopy. Nature. **352**:444-448.

Sheetz, M. C. Martenson (1991). Axonal transport: beyond kinesin and cytoplasmic dynein. Curr. Opin. Neurobiol. **1**:393-398.

Astumian, R.D. M. Brier. (1993). Fluctuations at work - Brownian ratchets and molecular motors.

Peskin, C., G. Odell G. Oster (1993). Cellular motions and thermal fluctuations: The Brownian ratchet. Biophys. J. **65**:316-324.

Svoboda, K., C.F. Schmidt, B.J. Schnapp S.M. Block (1993). Direct observation of kinesin stepping by optical trapping interferometry. Nature. **365**:721-727.

Ellis, R.J. (1993). Chaperonin duct. Nature. **366**:213-214.

Svoboda, K. S. Block (1994). Force and velocity measured for singel kinesin molecules. Cell.

Finer, J., R. Simmons J. Spudich (1994). Single myosin molecule mechanics: piconewton forces and nanometre steps. Nature. **368**:113-119.

Prost, J., J. Chauwin, L. Peliti A. Ajdari (1994). Asymmetric Pumping of Particles. Phys. Rev. Lett. **72**:1652-2655.

Peskin, C., B. Ermentrout G. Oster (1994). The correlation ratchet: A novel mechanism for generating directed motion by ATP hydrolysis. In: *Cell Mechanics and Cellular Engineering. V. C. Mow. F. Guilak, R. Tran-Son-Tay and R. Hochmuth* (ed). pp. New York: Springer-Verlag.

Doering, C., W. Horsthemke J. Riordan (1994). Nonequilibrium fluctuation-induced transport. Phys. Rev. Lett. **72**:2984-2987.